New replication technique for the fabrication of thin polymeric microfluidic devices with tunable porosity

J. de Jong, B. Ankoné, R. G. H. Lammertink* and M. Wessling

Received 30th June 2005, Accepted 9th September 2005
First published as an Advance Article on the web 28th September 2005
DOI: 10.1039/b509280a

In this article we present a new versatile replication method to produce thin polymeric microfluidic devices with tunable porosity. This method is based on phase separation of a polymer solution on a microstructured mold. Compared to existing microfabrication techniques, such as etching and hot embossing, our technique offers four advantages: (a) simple and cheap process that can be performed at room temperature outside clean room facilities; (b) very broad range of applicable materials (including materials that could not be processed before); (c) ability to make thin flexible chips; (d) ability to introduce and tune porosity in the chip. By introducing porosity, the channel walls can be used for selective transport of gasses, liquids and solutes. A proof-of-concept will be given, by showing fast CO_2 transport through the channel walls of a porous polymer chip. Furthermore, it will be demonstrated that the gas permeation performance of chips can be enhanced dramatically by a decrease in chip thickness and incorporation of porosity. We expect that the development of porous chips can lead to the on-chip integration of multiple unit operations, such as reaction, separation, gas liquid contacting and membrane emulsification.

1. Introduction

Nowadays, microfluidic devices gain attention from various disciplines. Many articles have already been published on the fabrication of these devices for unit operations such as reaction, separation, and analysis. This field of research is associated with Lab-on-a-chip and Micro Total Analysis Systems (μTAS). The history of μTAS, its principles and application have been described in an extensive review by the group of Manz.[1,2] Initially silicon and glass were used as the base chip material, but gradually new methods have been invented that allow for a broader material choice.[3] Replication techniques such as hot embossing and injection molding have enabled the use of several polymers.[4,5] For cheap rapid prototyping, PDMS and photo curable polymers are widely applied.[6] In two decades, the range of applicable materials has grown to a considerable amount. Strikingly, many articles deal with functionalization and coating of these materials after fabrication of the chip. The function of the chip material itself is in these cases limited to ''defining the microfluidic structure''. The question now arises: ''Would it not be more logical to choose a chip material that already *has* the required surface properties?'' Since the answer is obviously affirmative, it can be concluded that the material choice is still limited. This can be ascribed to limitations in the available production techniques.

A similar problem with limitations of production techniques is evident for the on-chip integration of multiple unit operations, a main focus point in microfluidics research.[7] At the moment, integration is mostly realized by (a) smart chip layout, (b) the introduction of additional materials and/or (c) the use of highly sophisticated equipment for post-treatment of chips. Examples are (a) the fabrication of a gas–liquid separator based on capillary forces;[8] (b) the preparation of membranes in a channel[9] and entrapment of absorption resins;[10] and (c) the fabrication of membranes by anodically etching[11] or laser beam drilling.[12] In all these cases, the properties of the chip material itself are hardly exploited.

Applied chip materials are dense, making transport of species through the chip material shear impossible. An exception is the transport of gasses or vapors through the walls of PDMS-based chips.[13] However, the permeation is low due to the significant thickness of the chips that is required for mechanical strength. The introduction of (interconnected) porosity in the chip material would lead to a big improvement. In a porous chip, the channel walls can act as selective barriers for transport of chemicals in- and out of the channel. This principle can be used to integrate different unit operations, *i.e.* membrane emulsification, gas–liquid contacting, liquid–liquid contacting, reaction, and separation. Another possibility to exploit the chip porosity is concentration of liquid streams by evaporation, a principle already reported by Timmer *et al.*[14] Also the practical problem of entrapment of air in microfluidic channels may be avoided. The benefit of porosity has been acknowledged by several authors, who applied porous *layers* in microfluidic chips. Examples are porous silicon for surface enhancement[15,16,17] and the incorporation of Teflon®,[14] silica,[18] polypropylene,[19] and polycarbonate membranes.[20] However, to our knowledge, the concept of porosity in the complete chip material *itself* has not yet been reported in the literature. When the use of porous materials is so promising, then why is porosity not directly incorporated? The answer might again be found in limitations of the existing fabrication methods.

University of Twente, Faculty of Science and Technology, Membrane Technology Group, P.O. Box 217, NL-7500 AE, Enschede, The Netherlands. E-mail: r.g.h.lammertink@tnw.utwente.nl; Fax: +31-53-489-4611; Tel: +31-53-489-2063

Summarizing, a method that is capable of introducing porosity into a microstructured film and additionally offers a broad variety of applicable materials has great potential. In 2002 such a technique was proposed: Phase Separation Micro Molding (PSμM).[21] This technique is based on phase separation of a polymer solution on a microstructured mold and has been described extensively by Vogelaar *et al.*[22,23] The technique has been demonstrated for many different polymers. When combined with a subsequent pyrolysis step, also carbon, metallic and ceramic films could be prepared.

In this article we will discuss the applicability of PSμM for the fabrication of porous microfluidic chips. The complete preparation process will be described, starting from film fabrication, *via* the sealing step to an operating porous assembly. The production of a multilayer chip will be demonstrated. A proof of principle of the added value of the introduced porosity will be given, by showing fast CO_2 transport *through* the channel walls. Finally, the gas permeation properties of produced porous films will be compared with dense films of the same material, and with PDMS, to demonstrate the enhancement by the porosity.

2. Background and aim

Phase separation or immersion precipitation is the general principle used for the fabrication of membranes and it is well described in the literature.[24] Phase separation occurs when a homogeneous polymer solution is brought into a supersaturated state and it leads to a spatial redistribution of the polymer. Subsequent fixation of the new distribution results in a polymeric matrix. The following three principles can be used to obtain a supersaturated polymer solution: (a) evaporation of the solvent; (b) change in temperature of the system or (c) introduction of a so-called 'non-solvent'. A non-solvent is a liquid that is miscible with the solvent of the polymer solution but immiscible with the polymer itself. The polymeric structures discussed in this article have been prepared by non-solvent induced phase separation. Therefore, some background on this process will be given.

The thermodynamic stability of a ternary system of polymer/solvent/non-solvent for all compositions is given by an isothermal phase diagram, such as depicted in Fig. 1. In region I, the system is thermodynamically stable, which means that the solution is homogeneous. Region II, enclosed by the binodal line, represents the compositions where the system is not stable. Here it can lower its free energy by separating in two liquid phases. This process is known as liquid–liquid demixing.

When a polymer solution is contacted with a non-solvent, its composition shifts and crosses the binodal line. The solution then becomes thermodynamically unstable and separates in a polymer-rich (a) and polymer-lean phase (b). The composition of both phases is given by the intersection points of the tie line and the binodal. Further exchange of solvent and non-solvent leads to gelation and solidification of the polymer rich phase. The porosity of the obtained polymer film stems from the polymer lean phase, which is removed by washing.

Vogelaar *et al.* found that when the phase separation process is carried out on a microstructured mold, the structure of the mold is replicated in the produced polymer film.[22] This process is schematically depicted in Fig. 2. First, a microstructured silicon mold is prepared. Then a polymer solution is cast on this mold. Phase separation is induced by immersion in a non-solvent bath. After release of the microstructured film, the mold can be cleaned and reused.

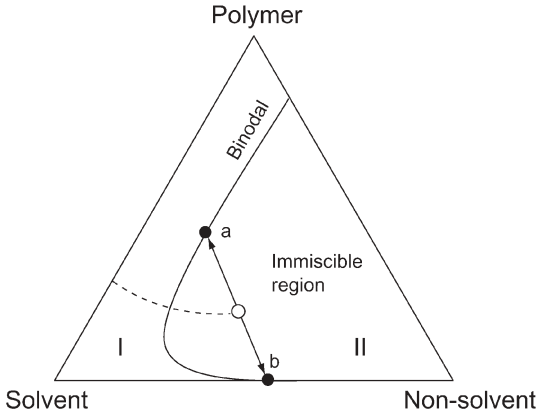

Fig. 1 Ternary phase diagram for a polymer/solvent/non-solvent system. Region I represents all compositions where the solution is homogeneous. Region II, enclosed by the binodal line, represents the unstable compositions where phase separation occurs in a polymer rich (a) and polymer lean phase (b).

The membrane characteristics of the microstructured film are defined by aspects of the morphology, such as pore size distribution, skin thickness, and surface/volume porosity. These parameters determine the *performance* of the membrane, which can be expressed in terms of permeability and selectivity. Phase separation can lead to three basic types of morphology: (1) completely dense structure; (2) porous substructure with

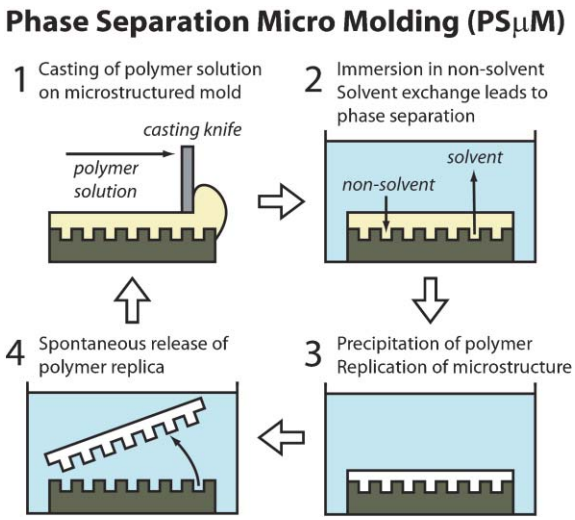

Fig. 2 Schematic representation of Phase Separation Micro Molding (PSμM). First a silicon microstructured mold is fabricated using standard clean room technology. A thin layer of a polymer solution is cast on this mold and subsequently immersed in a bath of non-solvent. Exchange of solvent and non-solvent leads to phase separation and the precipitation of polymer on the mold. During this process slight shrinkage occurs, causing the replica to detach from the mold spontaneously. After cleaning the mold can be reused.

dense skin layer; or (3) completely porous structure. The morphology that is obtained depends on the dynamic path in the ternary diagram that is followed during phase separation. This is related to a large range of parameters, including temperature, composition of the polymer/solvent/non-solvent system, casting thickness and pre-treatment prior to immersion (*e.g.* solvent evaporation, contact with non-solvent vapor). Since these conditions can be controlled, the final morphology can be tailored to suit the application. Pore sizes can range from 0 (dense) to several microns, covering separation processes from gas separation to microfiltration. The maximum achievable porosity is not limited by the process itself but rather by the mechanical stability of the obtained film.

During the formation of the polymeric matrix, shrinkage occurs that is intrinsic to the process. This shrinkage leads to a small gap between the mold features and the microstructured film. Release problems, as encountered in embossing, are therefore avoided. Due to this phenomenon, very thin films can be produced, down to a few microns. The size of the features can be even smaller, down to 150 nm.[22] The ability to make thin films enables the production of flexible chips.

A very significant advantage of phase separation micromolding is the enormous range of applicable materials; in principle, *any* soluble polymer can be used. Materials that are already reported include poly methyl methacrylate (PMMA), polycarbonate (PC), polystyrene (PS), poly vinyl difluoride (PVDF), polyimide (PI) (high Tg), polylacticacid (PLA) (biodegradable polymer) and polyaniline (conducting polymer).[23] When PSμM is combined with a subsequent pyrolysis step, carbon films can be prepared. Also inorganic films can be made, by adding ceramic (*e.g.* Al_2O_3) or metallic powder (*e.g.* silver) to the polymer solution and performing a pyrolysis and sinter step afterwards.[22] Thus, instead of tuning the surface of a standard chip material, now a material can be chosen that directly meets the requirements of the application.

Summarizing, Phase Separation Micro Molding offers the following opportunities: (a) ability to produce thin microstructured flexible films with (b) tunable porosity and (c) broad material choice, (d) in a simple and cheap process outside clean room facilities. The aim of this article is to show the applicability of PSμM for the fabrication of microfluidic chips. Furthermore we like to demonstrate that incorporation of porosity in the chip material itself can lead to a whole new range of possibilities for on-chip integration of multiple unit operations.

3. Experimental

3.1 Materials

Although the phase separation method can be used with many materials, in this article we have chosen the following 2 polymers as an example: Poly methyl methacrylate (PMMA, Mw 100 000, Polysciences) and acrylonitrile–butadiene–styrene copolymer (ABS, Magnum, high butadiene content, Dow Chemicals). These polymers were dissolved in either *N*-methyl-pyrrolidone (NMP, synthesis grade, Merck) or acetone (synthesis grade, Merck). Non-solvents were either tap water or ethanol (technical grade, Merck). Ecoline ink from Talens was used as a coloring agent. For the proof-of-concept of transport through the porous chip walls, acidification of water by CO_2 (Hoek Loos, 99.996% purity) was chosen. Bromo thymol blue (Aldrich) was dissolved in tap water and used as a pH indicator. All mentioned chemicals were used without additional pre-treatment.

3.2 Mold fabrication

Microstructured molds were produced in a clean room out of 4″ silicon wafers. The process consisted of standard photolithography, followed by deep reactive ion etching (DRIE). Several microfluidic designs were tested, all based on a channel width of 100 μm. The height of the rims on the mold was 50 μm.

3.3 Film casting

Film casting was performed at room temperature using a home made casting device. The height of the casting knife, and thereby of the resulting film, could be controlled by micromanipulators. After casting, the molds were either placed in the non-solvent bath directly or exposed to a nitrogen gas stream saturated with water vapor prior to immersion. Films were washed for 24 h in tap water to remove all remaining solvent and dried in air at room temperature before further processing. Since many different recipes and process conditions have been applied, we refer to the exact preparation procedure of films in the corresponding captions of figures.

3.4 Analysis and characterization methods

Produced replicas were analyzed by optical microscopy (Carl Zeiss Axiovert 40) and scanning electron microscopy (SEM, JEOL TSM 5600). Photographs were made with a Fujifilm Finepix 401 digital camera in the macro setting. Cross section samples were prepared by breaking wet films after immersion in liquid nitrogen. Before SEM analysis, a thin layer of gold was sputtered on prepared samples to avoid charge-up during imaging. Gas permeation measurements were performed in an in-home developed low pressure gas permeation set-up. Unstructured films were prepared by casting on a flat wafer. After washing for 24 h in tap water, the films were dried for 12 h in air and for 24 h in a vacuum oven at 30 °C. Permeation of carbon dioxide (Hoek Loos, 99.996% purity) was determined by measuring the pressure increase in time in a calibrated permeate volume at $T = 30$ °C, $P_{feed} = 1$ bar, $P_{permeate}$ = vacuum ($<10^{-5}$ bar).

3.5 Sealing

Produced films were sealed onto transparent PMMA cover slips that had been prepared by casting a thin film of 25 wt% PMMA/acetone solution on a glass plate. After evaporation of the acetone, the obtained flexible PMMA foil was removed and cut into small cover slips. Sealing was obtained by placing the films in a standard hot air oven at 80 °C for 6 min. During the sealing procedure, pressure was applied by clamping the films between microscope glass slides.

3.6 Assembly

For assembly testing, a pressure chip holder was used (Micronit Microfluidics, Enschede, The Netherlands). Glass

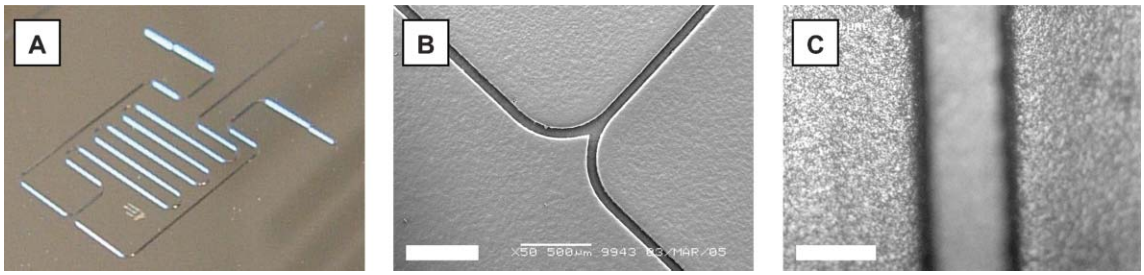

Fig. 3 Fabrication of porous microfluidic films: (A) photograph of a microfluidic design on a silicon mold; (B) SEM image of an ABS copolymer replica made by PSμM, showing a dense skin layer (bar represents 500 μm); (C) optical image of a close-up of a channel in the replica, revealing the porosity in the film beneath the skin (bar represents 100 μm). The depicted film was prepared from a 25 wt% solution of ABS in NMP using ethanol as non-solvent.

lids with powderblasted holes were used for the connection of capillaries. Both lids were coated with a thin polymeric film by casting a 5 wt% PMMA/acetone solution. In this way, better sealing was obtained between the glass lids and the porous film. After evaporation of the acetone, a porous microstructured film was sandwiched between the coated glass lids and sealed using the same sealing procedure as mentioned above. In this way, the channels of the chip consisted of a single material. The connections to reservoirs were pushed through prior to sealing. A Harvard Apparatus Picoplus syringe pump was used for liquid handling. Connections and silica glass capillaries were supplied by Upchurch Scientific.

4. Results and discussion

4.1 Film fabrication

Images of a typical mold design and resulting replicas made by PSμM are given in Fig. 3. The image obtained by SEM (B) shows a dense surface of the film and dense channel walls. The optical image (C) reveals the porous structure beneath the dense layer. As was mentioned in the background section, the morphology depends on the composition of the polymer starting solution and the conditions of the phase separation process. This is clearly demonstrated in the images of ABS films presented in Fig. 4. Different shapes and sizes of pores can be obtained. The final morphology can be predicted by rules-of-thumb available from the field of membrane preparation. Knowledge in this field is continuously expanding and already an enormous amount of recipes and resulting film morphologies has been documented.[24,25] This means that tailoring the morphology towards a certain application is rather straightforward.

An important phenomenon in Phase Separation Micro Molding is shrinkage of the film during exchange of solvent and non-solvent, in both lateral and perpendicular direction. Especially in perpendicular direction, large shrinkage can occur. This can be concluded when comparing the thickness of the films presented in Fig. 4 with the original casting thickness of the polymer solution. Starting out with 250 μm of solution, the final film thickness lies around 150 μm, which is 40% lower. The thickness of the final film is determined by (a) casting thickness, (b) polymer concentration and (c) the in-diffusion rate of non-solvent and out-diffusion rate of solvent during the phase separation process.

As can be seen in Fig. 4, the parameters of the phase separation process not only determine the morphology of produced films, but also the replication precision. In Fig. 4A, the sidewalls of the channel are slightly curved. We address this phenomenon to lateral shrinkage of the film *after* release from the mold. At the point of release still a lot of solvent is present in the film. During the washing step, the residual solvent is removed and shrinkage occurs. When the film is subsequently dried, further shrinkage can be observed. We have noticed that the shrinkage is specific for any polymer/solvent/non-solvent combination and the combination of applied process conditions in the phase separation process. Vogelaar *et al.* have already mentioned that shrinkage can also depend on the distance between features.[23] So on one side, shrinkage is beneficial as it causes a smooth release of the film from the mold, while on the other side it might cause undesired loss in feature sharpness. We have noticed that in general, shrinkage is in the order of 5–10% in the film–plane direction and uniform throughout the film. It is therefore straightforward to correct for this shrinkage in the original mold design.

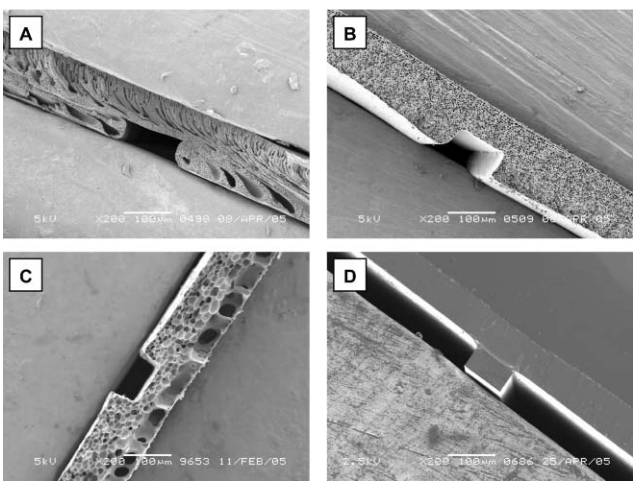

Fig. 4 SEM images of cross sections of structured films prepared from an ABS/NMP solution, cast at 250 micron, demonstrating the tunability of the film morphology: (A) 25 wt%, immersed in water; (B) 25 wt% immersed in ethanol; (C) 17 wt%, 5 min in water vapor before immersion in water; (D) close-up of cross section of the mold for comparison (all bars represent 100 μm).

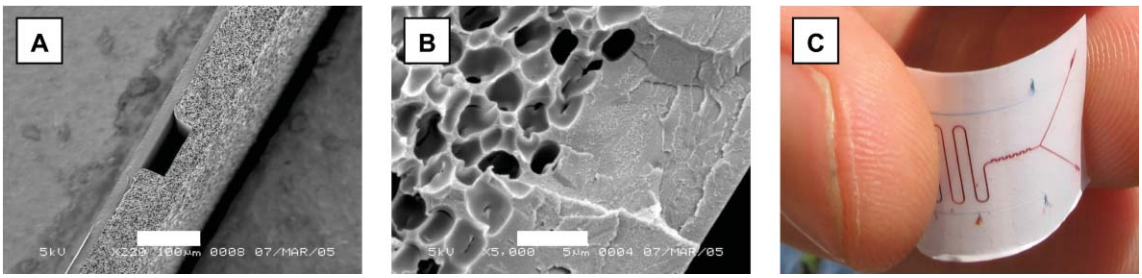

Fig. 5 Porous PMMA film sealed on dense PMMA layer: (A) cross section (bar represents 100 μm); (B) close-up of sealing interface, showing good cohesion (bar represents 5 μm); (C) demonstration of the flexibility of a sealed chip (channels have been wetted with ink by capillary forces to reveal the structure).

4.2 Sealing

In Fig. 5A, a cross section is given of a porous PMMA film sealed to a dense PMMA film. The close-up in Fig. 5B demonstrates very good cohesion; in fact, the interface between the two films has vanished. This means that no leakage occurs due to poor sealing. Films were still flexible after sealing, as is clearly illustrated in Fig. 5C. The white color of the chip stems from the porous microfluidic film; the dense polymer cover slip is transparent. This enables optical examination of the microfluidic device.

4.3 Assembly and operation

In order to operate the microfluidic structures and to demonstrate the benefit of introduced porosity, assembly into a module is required. We have decided to use a standardized module that is based on glass chips having powderblasted holes at standard positions. We have designed a mold with structures that fit onto these glass chips, taking effects of shrinkage into account. The module is schematically depicted in Fig. 6. In the same figure also a SEM image of a microfluidic film is given, together with an optical image of the chip resulting from this film in action. Although the bulk chip material was porous and some pores could be seen in the channel, we did not observe any fluid in the chip material itself, neither for the PMMA nor the ABS chips. Experiments with fluorescent markers also did not reveal any leakage or pore intrusion. However, we want to emphasize, that the chips discussed here only serve as an example of the possibilities of the replication method. As is known from membrane preparation also porous skins can be obtained.[24]

From the pictures in Fig. 5 and Fig. 6 it can be concluded that PSμM can be used to fabricate microfluidic chips. Since the method is suitable for a huge amount of materials (some yet unknown in microfluidics), PSμM seems to be a useful extension of the existing range of fabrication methods. Also the possibility to produce flexible films is very interesting. However, what really distinguishes the method from other available methods is the unique feature to directly introduce and tune porosity. We will therefore demonstrate the benefit of this feature, by exploiting the porosity for transport of gas through the chip walls into the microfluidic channels.

4.4 Proof of principle

For the proof-of-principle that the porosity can indeed be used for transport, we have chosen a simple reaction: the formation of carbonic acid in water. CO_2 is transported through the chip material by diffusion and dissolved in water flowing through the channels. This process leads to acidification of the water,

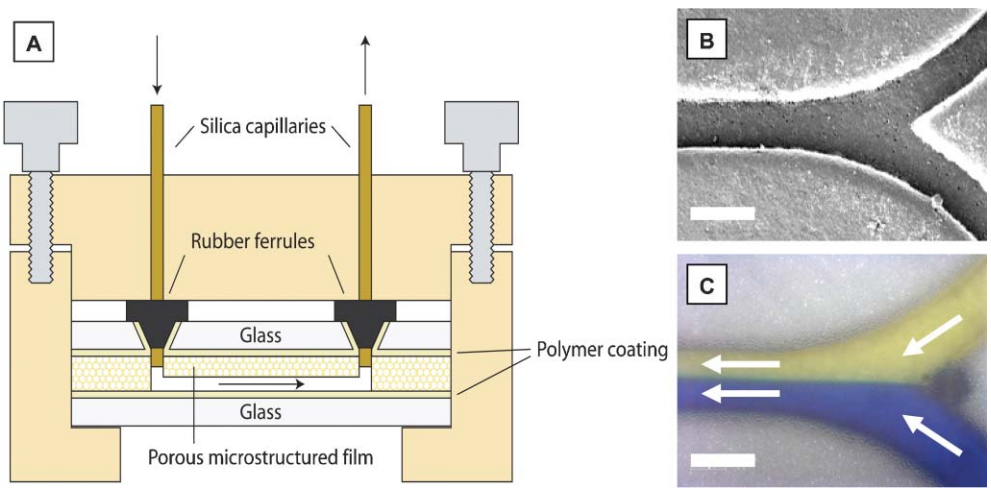

Fig. 6 (A) Schematic depiction of a chip assembled in the pressure chip holder; (B) SEM image of Y-joining element (bar represents 100 μm); (C) optical image of sealed Y joining element in action: joining of 2 water flows, colored with yellow and blue ink, clearly demonstrating laminar flow and a leak-free sealing (bar represents 100 μm, arrows indicate flow direction).

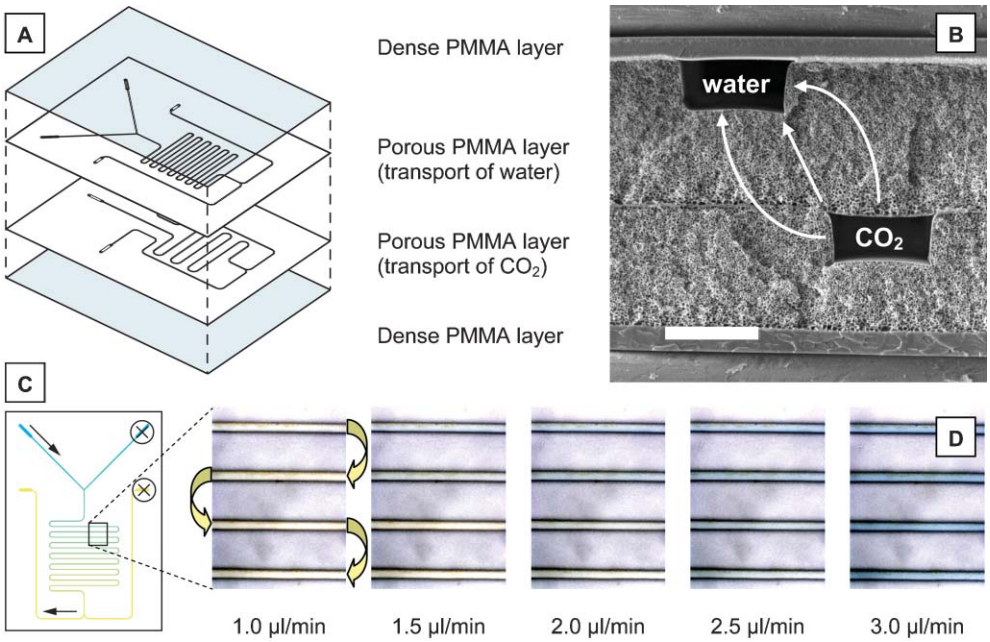

Fig. 7 Proof-of-principle of mass transport through the channel walls of a porous chip: (A) schematic chip assembly; (B) SEM image of a cross section of the sealed assembly (bar represents 100 µm), demonstrating the possibility to stack and seal multiple films; (C) schematic representation of acidification of water by CO_2 absorption, visualized by a pH indicator (blue at pH $>$ 7.8, yellow at pH $<$ 6.0); (D) optical images of the chip in operation, all taken at the same position (indicated by the area of interest in (C)). These pictures demonstrate fast CO_2 transport and show that the amount of CO_2 absorbed can be varied by the flow rate of the water stream.

which can be easily visualized with a pH indicator. To introduce water and CO_2 separately, a double-layered chip was prepared. The lay-out of this chip is illustrated in Fig. 7A. Two porous PMMA films were sealed between glass lids coated with a thin layer of PMMA as described before. The connections to reservoirs had been pushed through prior to sealing. A close-up of a cross section of the obtained assembly (without glass lids) is given in Fig. 7B. This picture clearly demonstrates the possibility to stack and seal *multiple* microfluidic layers.

Water containing a pH indicator was introduced by syringe pumping, while CO_2 was manually introduced with a syringe. No pressure gradient was applied, meaning that gas transport was governed by diffusion through the porous layer. The flow rate of the water phase was varied from 1 to 3 µl min^{-1} in order to vary the contact time. The results of the acidification experiments are presented in Fig. 7D. In case of CO_2 transport, the acidification would cause a color change of the pH indicator from blue (pH $>$ 7.8) to yellow (pH $<$ 6.0). Such a change is indeed visible in Fig. 7D. Therefore, we can state that the pictures provide a general proof that transport through the channel walls occurs. Furthermore, the amount of CO_2 absorbed can be regulated, and in this way a pH gradient can be set in the chip.

To further investigate the transport properties of produced films, gas permeation experiments were performed using CO_2. In this case the transport was not only driven by a concentration gradient, but also by a pressure gradient. From the gas permeation data the gas permeance of the film could be determined, which is defined as a flow normalized for surface area and applied pressure. The experimental results are presented in Table 1. The theoretical values for CO_2 permeance through *dense* films of similar thickness have been added, to demonstrate the effect of the porosity. These theoretical values can be calculated by dividing the permeability, a material dependent constant, by the film thickness. Looking at the calculated and measured values in Table 1, it is clear that porosity has an enormous enhancement effect on gas permeance. This can render materials with low permeability, such as PMMA, very competitive with highly permeable materials, such as PDMS. To illustrate this effect, the permeance value has been calculated for a PDMS chip with

Table 1 Comparison of calculated and measured CO_2 permeance through dense and porous films

Material	CO_2 permeability/ mol m m^{-2} s^{-1} Pa^{-1}	d_{film}/µm	$P_{calculated}$ [c] for dense film/ mol m^{-2} s^{-1} Pa^{-1}	$P_{measured}$ [d] for porous film/ mol m^{-2} s^{-1} Pa^{-1}	Enhancement by porosity
ABS	1.6×10^{-15} (ref. 26)	65[a]	2.5×10^{-11}	2.2×10^{-9}	~100
PMMA	1.1×10^{-16} (ref. 27)	150[b]	7.4×10^{-13}	3.8×10^{-8}	~50 000
PDMS	8.3×10^{-13} (ref. 25)	1000	8.3×10^{-10}	—	—

[a] 25 wt% ABS/NMP, coagulated in ethanol, casting thickness 200 µm. [b] 25 wt% PMMA/NMP, 5 min water vapor, coagulated in water, casting thickness 200 µm. [c] P = permeance, calculated by dividing permeability by the film thickness. [d] T = 30 °C, P_{feed} = 1 bar, $P_{permeate} < 10^{-5}$ bar.

Table 2 Possible applications of microfluidic films prepared by Phase Separation Micro Molding (PSμM), categorized by morphology type

Morphology	Film transparency	Permeable for	Mass transport	Possible applications
Completely porous	No	Gas, vapor, liquid, solutes, particles[a]	++	Liquid–liquid/gas–liquid contactor Supported liquid membranes Membrane emulsification Solute/particle/cell separation or concentration
Porous with dense skin	No	Gas, vapor	±	Easy degassing of chips (dehydration) Pervaporation Concentration by evaporation Gas–liquid contactor or separator Gas separation
Completely dense	Yes	Gas, vapor	—	Conventional microfluidics Optical applications

[a] Depending on pore size.

a typical thickness of 1 mm. The data is also enclosed in Table 1. The permeability of PDMS for CO_2 is around 500 or 7500 times higher than the values reported for ABS and PMMA, respectively. However, the *permeance* values for the porous PMMA and ABS films are both higher than the calculated value for the PDMS film. This difference is partly due to the lower film thickness, but mostly due to the enhancement effect of porosity. Only when the thickness of the PDMS membrane is lowered to 20 μm, which is state-of-the-art,[28] the permeance is equal to the porous PMMA. From the data in Table 1 an important conclusion can be drawn: the permeation performance of PDMS chips can be equaled or even surpassed by chips made out of materials with much lower permeability factors than PDMS, simply by making thinner chips and incorporating porosity.

The use of porosity for gas–liquid contacting might be an interesting alternative to two-phase gas–liquid flow, as is used in *e.g.* hydrogenation reactions in the group of Jensen.[16] Future research will involve a comparison between these two options, as well as optimization of the morphology of produced films. We will also explore the possibilities of fluid transport through the channel walls.

5. Outlook

Phase Separation Micro Molding is a new technology for the production of microfluidic chips and its features open up possibilities for improvement of existing chips and for completely new applications. A proof-of-principle for all these possibilities is beyond the scope of this article, but it is very interesting to philosophize about new research challenges. In Table 2 we have indicated several opportunities for the technology, categorized by the type of morphology. Stacking of films with different morphology can lead to even higher functionalities and the on-chip integration of multiple unit operations. Since the technique is both cheap and simple, we expect large benefits in scale-out towards industrial-sized applications and in the production of disposable chips.

6. Conclusions

In this article we have presented a new versatile replication method for the fabrication of porous microfluidic chips: Phase Separation Micro Molding (PSμM). We have demonstrated that PSμM can be used to fabricate microfluidic ABS copolymer and PMMA films, but many other polymers are possible as well. Release problems are avoided by small shrinkage in lateral direction that is intrinsic to the process. During phase separation, porosity is introduced and we have shown that this porosity can be tuned by varying the parameters of the process. Produced films can be sealed to a transparent cover slip by a combination of pressure and heat. The resulting sealed films are both thin and flexible and consist of only a single material. We have demonstrated that stacking and sealing of *multiple* layers is also possible. The performance of resulting microfluidic assemblies can be easily tested in a standardized module. A proof-of-concept of the benefit of the incorporated porosity has been given by showing fast CO_2 transport through the channel walls of a multi-layer chip. Finally, the gas permeation performance of chips can be enhanced dramatically by a decrease in chip thickness and incorporation of porosity. This enhancement is so strong that it enables low permeable materials to compete with PDMS, or even surpass its performance. The feature of porosity in the chip material opens up the way for on-chip integration of multiple unit operations. Summarizing, we can state that Phase Separation Micro Molding is a very promising extension of the existing range of microfabrication methods.

Acknowledgements

This research is part of the Dutch project "Process on a Chip" (PoaC). The Netherlands Organization for Scientific Research (NWO) is kindly acknowledged for financial support.

References

1 D. R. Reyes, D. Iossifidis, P. A. Auroux and A. Manz, *Anal. Chem.*, 2002, **74**, 2623–2636.★*This review provides a very good starting point for researchers new in the field of microfluidics*.
2 P. A. Auroux, D. Iossifidis, D. R. Reyes and A. Manz, *Anal. Chem.*, 2002, **74**, 2637–2652.
3 E. Verpoorte and N. F. de Rooij, *Proc. IEEE*, 2003, **91**, 6, 930–953.
4 L. J. Lee, M. J. Madou, K. W. Koelling, S. Daunert, S. Lai, C. G. Koh, Y. J. Juang, Y. Lu and L. Yu, *Biomed. Microdev.*, 2001, **3**, 4, 339–351.
5 M. Heckele and W. K. Schomburg, *J. Micromech. Microeng.*, 2004, **14**, R1–R14.★*Extensive historical overview of micromolding technologies, including a comparison and machine development*.

6 J. C. McDonald, D. C. Duffy, J. R. Anderson, D. T. Chiu, H. Wu, O. J. A. Schueller and G. M. Whitesides, *Electrophoresis*, 2000, **21**, 27–40.
7 D. Erickson and D. Li, *Anal. Chim. Acta*, 2004, **507**, 11–26.
8 A. Günther, S. A. Khan, M. Thalmann, F. Trachsel and K. F. Jensen, *Lab Chip*, 2004, **4**, 278–286.
9 H. Hisamoto, Y. Shimizu, K. Uchiyama, M. Tokeshi, Y. Kikatuni, A. Hibara and T. Kitamori, *Anal. Chem.*, 2003, **75**, 350–354.
10 K. Sato, M. Tokeshi, T. Odake, H. Kimura, T. Ooi, M. Nakao and T. Kitamori, *Anal. Chem.*, 2000, **72**, 1144–1147.
11 R. W. Tjerkstra, J. G. E. Gardeniers, J. J. Kelly and A. van den Berg, *J. Microelectromech. Syst.*, 2000, **9**, 4, 495–501.
12 S. Metz, C. Trautmann, A. Bertsch and Ph. Renaud, *J. Micromech. Microeng.*, 2004, **14**, 324–331.
13 E. Verneuil, A. Buguin and P. Silberzan, *Europhys. Lett.*, 2004, **68**, 3, 412–418.
14 B. H. Timmer, K. M. van Delft, W. Olthuis, P. Bergveld and A. Van den Berg, *Sens. Actuators B*, 2003, **91**, 342–346.
15 J. Drott, K. Lindström, L. Rosengren and T. Laurell, *J. Micromech. Microeng.*, 1997, **7**, 14–23.
16 M. W. Losey, R. J. Jackman, S. L. Firebaugh, M. A. Schmidt and K. F. Jensen, *J. Microelectromech. Syst.*, 2002, **11**, 6, 709–717.
17 D. Clicq, R. W. Tjerkstra, J. G. E. Gardeniers, A. van den Berg, G. V. Baron and G. Desmet, *J. Chromatogr. A*, 2004, **1032**, 185–191.
18 R. S. Foote, J. Khandurina, S. C. Jacobson and J. M. Ramsey, *Anal. Chem.*, 2005, **77**, 1, 57–63.
19 X. Wang, C. Saridara and S. Mitra, *Anal. Chim. Acta*, 2005, **543**, 1–2, 92–98.
20 R. F. Ismagilov, J. M. K. Ng, P. J. A. Kenis and G. M. Whitesides, *Anal. Chem.*, 2001, **73**, 5207–5213.
21 C. J. M. van Rijn, L. Vogelaar, W. Nijdam, J. N. Barsema and M. Wessling, *patent application WO0243937*, 2002.
22 L. Vogelaar, J. N. Barsema, C. J. M. van Rijn, W. Nijdam and M. Wessling, *Adv. Mater.*, 2003, **15**, 1385–1389.★*This is the first article about Phase Separation Micromolding, discussing the principle in more detail.*
23 L. Vogelaar, R. G. H. Lammertink, J. N. Barsema, W. Nijdam, L. A. M. Bolhuis-Versteeg, C. J. M. van Rijn and M. Wessling, *Small*, 2005, **1**, 6, 645–655.★*This article reviews many different materials that can be processed with Phase Separation Micromolding, including recipes. Furthermore the issues of shrinkage and minimal achievable feature sizes are addressed.*
24 M. Mulder, *Basic principles of membrane technology*, Kluwer Academic Publishers, Dordrecht, The Netherlands, 2nd edn, 1996.★*This book is a standard in the field of membrane technology, discussing membrane materials, membrane preparation and characterization, applications, thermodynamics and modeling.*
25 R. W. Baker, *Membrane technology and applications*, John Wiley & Sons, New York, 2nd edn, 2004.
26 *Permeability and other film properties of plastics and elastomers*, Plastics Design Library, New York, 1995.
27 C. T. Wright and D. R. Paul, *Polymer*, 1997, **38**, 8, 1871–1878.
28 A. P. Vollmer, R. F. Probstein, R. Gilbert and T. Thorsen, *Lab Chip*, 2005, **5**, 1059–1066.